

A GPS-Based Attitude Determination System for Small Satellites

Daniel Gershman, Kristopher Young,
Anders Kelsey, Ofer Eldad, Jason Rostoker,
Shan Mohiuddin, Alessandro Cerruti, Mason Peck,
Cornell University Space Systems Labs
155 Rhodes Hall, Ithaca, NY 14853
djg52@cornell.edu, khy6@cornell.edu,
aak26@cornell.edu, oe23@cornell.edu, jer44@cornell.edu,
sm386@cornell.edu, apc20@cornell.edu, mp336@cornell.edu

Abstract:

This paper presents a novel, GPS-based attitude determination system (ADS). Carrier-phase differential GPS (CDGPS) accurate to within centimeters enables magnetometer-level pointing accuracy. Employing three GPS antennas allows for the determination of three independent baseline vectors, which can be combined to yield a precise attitude solution. Both simulation data for a satellite in LEO and terrestrial field test data suggest sub-centimeter level accuracy, yielding an instantaneous pointing accuracy of approximately 2 degrees. This high precision makes possible numerous navigation-sensitive applications, such as in-orbit inspection, construction, or repair. Such technology offers many advantages to a small satellite system. Most significantly, a GPS-based ADS offers a high performance-to-cost ratio and requires minimal calibration, providing an ideal solution for small satellites. CUSat, an entry into the University Nanosatellite-4 competition, is a technology demonstrator for GPS-based attitude determination and provides a pointing accuracy better than 5 degrees. The CUSat CDGPS-based ADS provides a complete solution for high precision attitude determination and navigation with a simple interface and modular design.

Nomenclature

$t_{A_{k_0}}$ initialization time for receiver A
 $t_{A_0^j}$ time receiver A starts tracking satellite j (seconds)
 $t_{A_k^j}$ time k in receiver A
 t_e GPS epoch time (seconds)
 ϕ carrier phase measurement (cycles)
 η accumulated phase of L1 replica signal between times k and $k-1$. (cycles)
 ψ accumulated phase of incident signal between times k and $k-1$. (cycles)
 Γ^j fractional part of γ^j (cycles)
 Φ integrated carrier phase (cycles)
 Γ_e^j fractional phase transmitted by satellite j at GPS epoch (cycles)
 γ^j accumulated phase of transmitted L1 by satellite j (cycles)
 $N_{A_P}^j$ unknown integer number of cycles between satellite j and receiver A (cycles)
 N_A^j phase ambiguity (cycles)
 ρ true range (meters)
 λ_{L1} wavelength of nominal L1 signal (meters)
 δ_k^j clock error of satellite j at time k (seconds)
 δ_{A_k} clock error of receiver A at time k (seconds)
 P measured pseudorange (meters)
 Z residual error (meters)
 e_k noise
 Subscripts: A_{k_0} corresponds to time $t_{A_{k_0}}$
 A_0^j corresponds to time $t_{A_0^j}$
 A_k^j corresponds to $t_{A_k^j}$

e corresponds to t_e

Q direction cosine matrix
Pre sup coordinate frame transferring to
Post sup Coordinate frame transferring from
 R vector between antennas
 r CDGPS generated relative vector
 B Davenport's attitude matrix
 \hat{x} estimate of variable x

1. Introduction

An attitude determination system (ADS) based on a GPS sensor suite offers distinct advantages over traditional attitude determination methods for small spacecraft. Such a system greatly simplifies many of the common challenges encountered during the implementation of an ADS. The proposed system provides a method of attitude determination that has instantaneous accuracy to within 2 degrees for a roughly 0.5m diameter spacecraft, while simultaneously offering an independent calibration, broadly applicable, low-cost solution suited to the unique demands of small spacecraft. Implementation of this system yields magnetometer-level accuracy without the need to manage a magnetic-field model and contend with the

spacecraft's own magnetic moment. It offers sun-sensor accuracy even in eclipse. These benefits come at the cost of the higher processing load represented by the algorithms, but on-board processing represents less of a driver now than at any time in the past.¹

A GPS-based ADS is independent of orbital inclination in LEO, in contrast to common technologies such as earth sensors, sun sensors, star trackers and magnetometers. Such devices require specific calibration, placement, and orientation on the spacecraft to accommodate the prescribed orbit. The hardware and software architecture is modular and independent of the application. The system described requires only that three small antennas be placed on the satellite surface.

Of particular interest is Carrier-phase Differential GPS (CDGPS), which provides sub centimeter-level accuracy. A CDGPS driven ADS offers a high performance-to-cost ratio. High pointing accuracy can be provided without expensive hardware, such as star trackers. Although such devices can offer highly accurate attitude determination, they are accompanied by prohibitive multi-million dollar prices.² As a major objective of small satellite programs is often cost minimization, the economical GPS ADS solution is well suited for such applications. Moreover, the CDGPS hardware can easily support multi-body relative attitude determination and ranging operations, further increasing the value-added of such a system.

The particular CDGPS implementation discussed has advantages over previous algorithms.³ Each iteration of this algorithm executes quickly allowing for rapid convergence and real-time execution. In this implementation CDGPS is used to generate relative baseline vectors for attitude determination and relative navigation. Using these baseline vectors, an attitude estimator can be used to determine both relative and absolute attitude. The CDGPS and attitude determination overview provides context to the discussion of design considerations and mission requirements such as antenna placement, orbital parameters and pointing requirements.

The Cornell University Satellite (CUSat) project is used as a case study for a GPS based ADS. CUSat is an end-to-end autonomous in-orbit inspection system that utilizes CDGPS to provide relative orbit and attitude information. The two spacecraft will take visual spectrum data at a range of several meters. The CUSat discussion addresses the design considerations highlighted in this paper in the context of its missions. Although this particular discussion is applied to small satellite missions, the technology described is scalable to any Low Earth Orbit (LEO) mission.

2. GPS Overview

GPS satellites transmit a carrier signal at L1 (1.57542 GHz) modulated by a Coarse Acquisition (C/A) code at 1.023 MHz. The C/A code repeats every 1ms. Most commercial GPS receivers use the measured phase of the C/A code to generate pseudorange observables. Pseudoranges from four or more satellites can be used to calculate a 3-D navigation solution accurate to within several meters. When very accurate relative position is required or when large data sets can be post-processed, the measured carrier phase of the signal can be used to obtain more accurate positioning.

2.1. GPS Observables

The C/A code has a nominal length of approximately 300m while the L1 carrier signal has a nominal wavelength of approximately 19cm. A typical commercial receiver can measure code phase or carrier phase to within 1%. Therefore, the maximum possible range measurement accuracy is $0.01 \cdot \lambda$. This accuracy corresponds to about 3m for a code phase based range measurement and 2mm for a carrier phase based range measurement.⁴ These values represent the lower bound on ranging errors due to multipath and thermal noise since satellite geometry and ephemeris, ionosphere, and troposphere ranging errors will contribute to the overall navigation solution error.

Since the C/A code repetitions are aligned to the GPS second, the transmitted phase of the C/A code at a given time is predictable, allowing for unambiguous pseudoranges to be generated. However, the phase of the transmitted carrier signal is not predictable for a given time. Therefore, there will be phase ambiguities, or biases, inherent in carrier phase measurements, which must be resolved before a navigation solution can be obtained.

2.2. Differential GPS

If only the relative vector between two GPS antennas is required, Differential GPS (DGPS) measurements may be used. Applications for such measurements include relative position control of satellite formations, inspection and docking maneuvers and both absolute and relative attitude determination for one or more spacecraft. Differential measurements yield more precise results than differencing absolute positions directly, due to the cancellation of errors common to both measurements used in the difference. Two widely used DGPS methods of eliminating these so-called common errors are single differencing and double differencing.

A single-differenced measurement can be generated if two receivers track the same, single GPS satellite, eliminating common errors such as ephemeris, satellite clock errors, and large-scale ionospheric and tropospheric errors. By differencing two single differences, a double-differenced measurement is created. In addition to eliminating common errors, a double-differenced measurement removes oscillator drift and receiver clock errors. Double-differenced measurements can be generated if two receivers are tracking the same two GPS satellites.⁴

The CDGPS algorithm implemented uses double-differenced carrier-phase measurements.⁵ The carrier-phase ambiguities mentioned previously are not eliminated in the double difference. However, in this approach it is not necessary to resolve each phase ambiguity individually; only the double differenced phase ambiguities have to be resolved. Moreover, if these ambiguities can be guaranteed to be integers, their resolution is simplified, enabling real-time relative navigation with current on-board processing technologies. While single-differenced carrier-phase ranging equations can be used to obtain a relative-navigation solution, the resolution of the single-differenced phase ambiguities is not trivial and the solution can require minutes of data to converge.

3. Carrier-Phase Measurements

This section provides an overview of generating true double differenced integer ambiguities. This discussion motivates the advantages of the applied CDGPS algorithm. The technique described is explained in detail by *Psiaki and Mohiuddin, 2005*.⁶

The relative motion between a receiver and satellite causes a Doppler shift on the received signals. To accurately track a satellite, a GPS receiver generates a replica signal at the appropriate Doppler-shifted frequency and phase as the incident signal. Receivers also generate a replica signal at the nominal L1 frequency to use as a reference. Integrated carrier phase is a measure of the beat phase of the two replicas, making it a measurement of integrated Doppler.⁷

When a receiver (A) locks onto a satellite (j) at time t_{Ao}^j , it measures the Doppler phase shift of the incident signal, initializing the carrier-phase measurement as

$$\phi_{Ao}^j = \eta_{Ao}^j - \psi_{Ao}^j \quad (1)$$

where η_{Ao}^j is the fractional phase of the L1 replica at time t_{Ao}^j and ψ_{Ao}^j is the measured fractional phase of the incident signal at time t_{Ao}^j .

The measured carrier phase is accumulated in subsequent time steps (k) as

$$\phi_{Ak}^j = \eta_{Ak}^j - \psi_{Ak}^j + \phi_{A(k-1)}^j \quad (2)$$

Each GPS satellite broadcasts a fractional phase of the L1 carrier signal (Γ_e^j) at GPS epoch time (t_e). This time is the same for all GPS satellites to within the accuracy of the GPS satellite clocks. The accumulated phase of the L1 signal from time t_e to time step k is

$$\gamma_{Ak}^j = \Gamma_e^j + f_{L1} \cdot (t_{Ak}^j - t_e) \quad (3)$$

The receiver generated L1 replica signal will not be perfectly phase-aligned to the L1 signal broadcast by a given GPS satellite. In addition, replicas in different receivers will have different offsets. In order to obtain meaningful measurements, all channels on all receivers should use the same L1 reference signal. Accomplishing this goal requires that a fractional offset be subtracted from the measured integrated carrier phase. This removes the initial phase (η_{Ao}^j) of the L1 replica in the receiver at time t_{Ao}^j , and replaces it with the fractional phase (Γ_{Ao}^j) that the satellite broadcasts at t_{Ao}^j .

Therefore, the integrated carrier phase is defined as

$$\Phi_{Ak}^j = \phi_{Ak}^j - (\eta_{Ao}^j - \Gamma_{Ao}^j) \quad (4)$$

With the addition of the term $\eta_{Ao}^j - \Gamma_{Ao}^j$, the proper L1 reference is used for all channels on all receivers. Φ_{Ak}^j is not a measurable value.

3.1. Ranging

A carrier-phase measurement is useful only when it can be included as an observable. It has been shown by *Kintner, 2005*, that the range from GPS satellite j to receiver A is

$$\rho_{Ak}^j = \lambda_{L1} (\Phi_{Ak}^j + N_{Ap}^j) + c(\delta_k^j - \delta_{Ak}^j) + e_k \quad (5)$$

When the receiver initially locks onto a satellite, there exists an integer number and fractional number of carrier cycles between the receiver and satellite.⁶ Both quantities differ for every satellite. The integer number of carrier cycles (N_{Ap}^j) is called the integer ambiguity. In the absence of cycle slips, the integer ambiguity

stays constant while a receiver tracks a satellite. The fractional phase is represented by the $\eta_{Ao}^j - \Gamma_{Ao}^j$ term in Φ_{Ak}^j . These terms can be combined to form a phase ambiguity (N_A^j) which is not an integer

$$N_A^j = N_{Ap}^j - (\eta_{Ao}^j - \Gamma_{Ao}^j). \quad (6)$$

Recall that it is not possible to measure Φ_{Ak}^j effectively; only ϕ_{Ak}^j can be measured. The ranging equation must be rewritten in terms of ϕ_{Ak}^j yielding

$$\rho_{Ak}^j = \lambda_{L1} (\phi_{Ak}^j + N_A^j) + c(\delta_k^j - \delta_{Ak}^j) + e_k. \quad (7)$$

The phase ambiguity biases carrier-phase measurements. This bias must be resolved before the range can be determined. In the case of real-valued biases, this problem can be computationally expensive, requiring minutes of data before converging to the correct value. However, if these biases can be guaranteed to be integers, the problem becomes much simpler as the search space is greatly reduced, allowing for real-time relative navigation, even recovery from a lost-in-space condition.

3.2. Carrier-Phase Differential GPS (CDGPS)

If three-axis attitude is to be determined, two baseline vectors must be measured and/or known simultaneously in both coordinates of the spacecraft body and the reference coordinates. To generate these vectors, more accurate differential techniques can be used.

3.2.1. Single Differencing

The single-difference technique can be applied when two nearby receivers are each tracking at least five mutually visible satellites. A single-differenced measurement is the difference between the carrier phase on two different GPS receivers (A and B) tracking the same satellite (j).

In general, the single difference is defined as

$$\Delta(\diamond)_{ABk}^j \equiv (\diamond)_{Ak}^j - (\diamond)_{Bk}^j, \quad (8)$$

where \diamond is the quantity being single-differenced. Hence, the single differenced integrated carrier phase is

$$\Delta\Phi_{ABk}^j = \Delta\phi_{ABk}^j - \Delta\eta_{ABo}^j + \Delta\Gamma_{ABo}^j. \quad (9)$$

Assuming receivers A and B are within about 1km, ephemeris, satellite clock, and large-scale ionospheric

and tropospheric errors measured from satellite j are canceled out in the single difference.⁴

Then, the single-differenced range equation becomes:

$$\Delta\rho_{ABk}^j = \lambda_{L1} (\Delta\phi_{ABk}^j + \Delta N_{ABp}^j) + e_k. \quad (10)$$

At this point the single differenced phase ambiguity, ΔN_{AB}^j is still not an integer.

3.2.2. Double Differencing

A relative-navigation solution can also be found using a double-differenced technique. Double differences are composed of two single differences and still require five mutually tracked satellites. A double-differenced measurement is the difference between the carrier phase on two different GPS receivers (A and B) tracking the same two satellites (i and j).

It follows that the double difference can be defined as

$$\nabla\Delta(\diamond)_{ABk}^{ij} \equiv \Delta(\diamond)_{ABk}^i - \Delta(\diamond)_{ABk}^j. \quad (11)$$

Then, the double differenced integrated carrier phase becomes

$$\nabla\Delta\Phi_{ABk}^{ij} = \nabla\Delta\phi_{ABk}^{ij} - \nabla\Delta\eta_{ABo}^{ij} + \nabla\Delta\Gamma_{ABo}^{ij}. \quad (12)$$

In this result the oscillator drift and receiver clock offsets, which are common to all channels on a receiver, are eliminated in addition to common errors.

3.2.2.1. Integer Ambiguities

Through receiver design detailed by *Psiaki and Mohiuddin, 2005*, the fractional phase of η can be guaranteed to be the same for all time steps.⁶ In addition, the same replica signal can be used for all channels. Under these assumptions,

$$\eta_{Ak}^i = \eta_{Ak}^j \quad (13)$$

$$\eta_{Ak}^j = \eta_{Ao}^j = \eta_{Ako}^j, \quad (14)$$

where η_{Ako}^j is the fractional phase of the L1 replica when the receiver is initialized. It follows that

$$\nabla\Delta\eta_{ABo}^{ij} = 0. \quad (15)$$

The transmitted L1 signal is offset from the receiver L1 replica, but accumulates the same amount of phase in a

given time interval. Therefore, if η_{Ako} is the same for all time steps in a receiver, then Γ_{Ako} is the same for all time steps in a receiver, yielding

$$\Gamma_{Ak}^j = \Gamma_{Ao}^j = \Gamma_{Ako}^j. \quad (16)$$

The fractional phase (Γ), unlike η , is different for each channel, due to the unknown phases Γ_e^i and Γ_e^j as shown in Equations 17 and 18.

$$\Gamma_{Ako}^i - \Gamma_{Ako}^j = \Gamma_e^i - \Gamma_e^j \quad (17)$$

$$\Gamma_{Bko}^i - \Gamma_{Bko}^j = \Gamma_e^i - \Gamma_e^j \quad (18)$$

Because Γ_e^i and Γ_e^j are receiver independent the double differenced quantity becomes

$$\nabla\Delta\Gamma_{ABko}^{ij} = \nabla\Delta\Gamma_{ABo}^{ij} = 0. \quad (19)$$

Both η and Γ drop out in the double difference making the double differenced phase ambiguity

$$\nabla\Delta N_{AB}^{ij} = \nabla\Delta N_{AB\rho}^{ij}, \quad (20)$$

which is guaranteed to be an integer. The double-differenced range equation is therefore

$$\nabla\Delta\rho_{ABk}^{ij} = \lambda_{L1}(\nabla\Delta\phi_{ABk}^{ij} + \nabla\Delta N_{AB\rho}^{ij}) + e_k. \quad (21)$$

Since the directions from receivers A and B to satellites i and j are known from the code-based navigation solution and the ephemerides, two receivers tracking at least five common satellites can utilize double-differenced carrier phase measurements. This yields relative-navigation solutions of sub-centimeter level accuracy.⁴ Since the double-differenced carrier phase bias is guaranteed to be an integer, real-time relative navigation is possible.

4. CDGPS Algorithm

The CDGPS algorithm used on CUSat takes advantage of the integer nature of the double differenced phase ambiguity, $\nabla\Delta N_{AB}^{ij}$.³ Because the double-differenced ambiguities are assumed to be integers instead of real numbers, the search space for the proper $\nabla\Delta N_{AB}^{ij}$ is greatly reduced. A reduced search space allows for faster algorithm convergence times, enabling real-time navigation.

Other double-difference algorithms can require several minutes of data to obtain a relative navigation solution, whereas the integer technique can require only seconds.³ In fact, when treated as real numbers, and in terrestrial applications, the ambiguity estimates may take as long as 25-30 minutes to converge to numbers close enough to safely round to integers. The Least-squares Ambiguity Decorrelation Adjustment (LAMBDA) method is used to solve for the integer ambiguities in a given search space.⁸ The size of this search space determines the convergence time of the algorithm.³

To reduce the phase ambiguity search space further, the algorithm makes use of pseudorange measurements in the receivers. The relationship between the true range, ρ_{Ak}^j to the measured pseudorange, P_{Ak}^j is

$$\rho_{Ak}^j = P_{Ak}^j - c(\delta_k^j - \delta_{Ak}) + e_k. \quad (22)$$

The receiver clock offset (δ_{Ak}) is calculated as part of the navigation solution and represents only an estimate of the true clock error. There is also error due to receiver noise. As a result, every channel of a receiver experiences residual error.

The residual error, Z_{Ak}^j , is

$$Z_{Ak}^j = \rho_{Ak}^j - [P_{Ak}^j - c(\delta_k^j - \delta_{Ak})] \neq 0. \quad (23)$$

The code solution provides an estimate of the line-of-sight vector from a receiver to a GPS satellite. The residual error provides a range in this direction, centered about the code solution, within which the true position lies. Using the residual error range, the search space is further reduced by providing tighter bounds for the integer ambiguity.⁵

Figure 1 demonstrates how the ambiguity search space can be narrowed by assuming true integer ambiguities and considering residual errors. This figure does not depict the actual process of resolving the double differenced ambiguities.

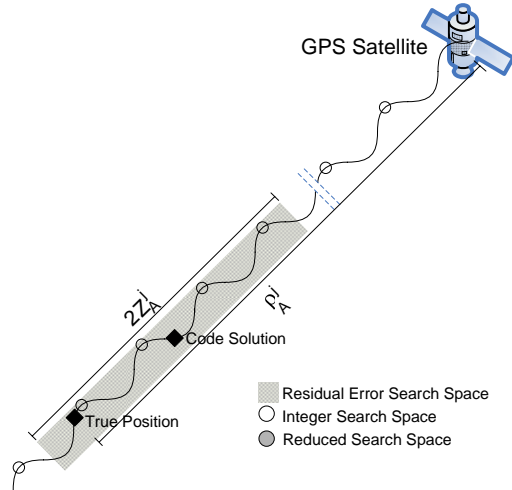


Figure 1. Simplified Ambiguity Search Space

(Adapted from Fig. 1 in *Psiaki and Mohiuddin, 2005*³)

While not implemented in the current algorithm, the search space for an attitude determination system can be further reduced by using the known fixed distances between antennas.⁴ In addition, the algorithm has a robust cycle-slip recovery mode, which detects and mitigates the effect of carrier cycle slips in a GPS receiver.⁵ The algorithm can also handle the periodic addition and removal of satellites to the CDGPS solution without needing to reconverge.

4.1. Solution Convergence

CDGPS requires that the differences in line-of-sight vectors between receivers and GPS satellites are not close to zero. The time rate of change of those vectors must also be not close to zero. The resolution of double-differenced ambiguities relies on the constancy of the integer ambiguities while the receivers are tracking GPS satellites. The changes in the measured carrier phase over time are used to determine the integer ambiguities. If the line-of-sight vectors and their time derivatives are too similar, it is difficult to resolve the ambiguities.⁴

In addition, if errors in phase measurements become too severe, they can cause the double-differenced ambiguities to deviate from integer values, making convergence impossible.⁴

Several situations can impede the ability of the algorithm to determine the integer ambiguities.⁹ Examples include dilution of precision (DOP), multipath, line of sight vector dynamics, signal power, residual errors, the ionosphere, and cycle slips.

High Geometric Dilution Of Precision (GDOP) implies that the satellite geometry as observed from the receiver is poor. Poor geometry corresponds to a difference between line of sight vectors for two or more satellites that is close to zero.

Multipath errors arise when nearby obstacles reflect the signal back toward the antenna. The arrival time of reflected signals is delayed with respect to the direct signal. If the delay between the direct signal and the reflected signal is less than $1\mu\text{s}$, measurement errors will occur. This interference makes accurate measurement of carrier phase difficult.

For a stationary receiver, certain GPS satellites may appear stationary in the sky for periods of time. This causes the change in line-of-sight vectors to be close to zero from one measurement to the next.

A receiver can measure carrier phase more accurately when the carrier-to-noise ratio is high. A low carrier-to-noise ratio implies that the carrier signal is buried in the noise. Therefore, errors in the measured number of carrier cycles are more likely.

If the residual errors of the pseudorange solutions are large (as a consequence of high dilution of precision and multipath), the search space of integer ambiguities is widened, making it more difficult to resolve them.

Propagation through the ionosphere can cause issues with measuring carrier phase on a receiver. This problem is most severe for low-elevation satellites. However, for short baselines, most ionospheric effects are double differenced out.

Cycle slips occur when the receiver loses carrier lock on a satellite for brief periods of time. When the receiver reacquires carrier lock on the satellite, an integer number of half cycles has been ignored, causing the phase ambiguities to change. In this case, the double-differenced phase ambiguities must be recomputed.

4.2. LEO Considerations

A LEO environment mitigates many of the convergence issues considered. LEO is a low-multipath environment, where the only possible reflections are off nearby spacecraft or off the host spacecraft. Furthermore, the high velocity of the spacecraft ensures rapidly changing line of sight vectors. More satellites may be visible than in a given terrestrial environment, ensuring a low GDOP. As a result, it is possible to obtain very fast convergence times for CDGPS in LEO.⁵

4.3. Results

The results presented in this section were obtained from tests using the Cornell University GPS Autonomous Receiver (COUGAR), which has been modified in house to generate true integer double differenced phase ambiguities.⁶

Two AN-10SC GPS patch antennas from Synergy Systems were mounted with the same orientation on an aluminum plate, placed 23.6 cm apart. GPS data was the recorded. Figure 2 shows the CDGPS error magnitude results of this terrestrial field test.

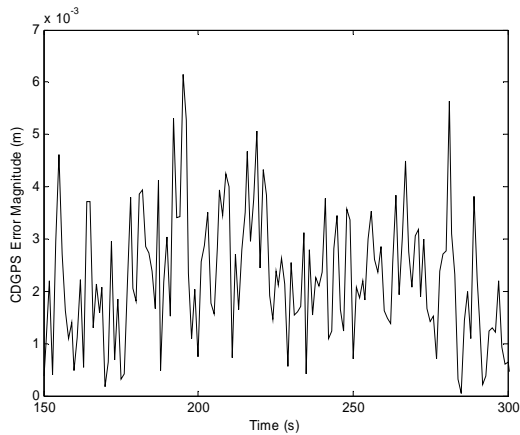


Figure 2. Terrestrial Field Test - Short Baseline

This data required 150 seconds to converge due to the terrestrial environment and multipath, but demonstrates that real-time CDGPS is possible. Real data can then be used to verify LEO simulations.

As discussed in Section 4.1, a LEO environment should provide faster convergence. Figure 3 shows the convergence time of a CDGPS solution in a simulated LEO environment. The same GPS observables were used for each curve, but the number of GPS satellites used in the solution was varied. Changing the number of GPS satellites implies a change in GDOP as well as a change in the line of sight dynamics. Note that with a sufficient number of GPS satellites, it is possible for convergence in a single time step.

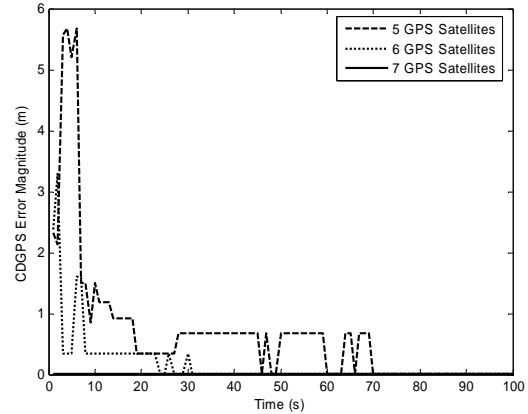


Figure 3. CDGPS Convergence Time

Figure 4 shows the CDGPS error magnitude for the LEO simulation.

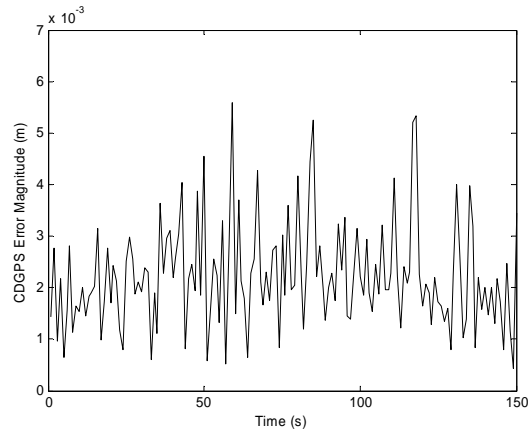


Figure 4. Simulated LEO Data - Short Baseline

Both the simulated and real data show mean errors on the order of millimeters and a maximum error less than 1 cm. Data statistics for both plots are listed in Table 1.

Table 1. CDGPS Data Statistics

Test	Mean Error (cm)	Std. Dev Error (cm)
LEO Simulation	0.22	0.1
Terrestrial	0.19	0.12

5. Attitude Determination

CDGPS will provide CUSat's attitude determination algorithm with relative vectors between two antennas in the standard GPS Earth Centered Earth Fixed (ECEF) coordinate system. These vectors are then transformed, using a Direction Cosine Matrix (DCM) ${}^{ECI}Q^{ECEF}$, into

Earth Centered Inertial (ECI, or inertial) reference coordinates. This transformation is known very precisely when the GPS code solution is available. In the rare absence of the code solution, an orbit propagator updates this rotation matrix. ECI is chosen as the attitude estimation reference coordinates, as it fixes the physics of the orbit and is independent of a particular application, providing a more general result.

At least two baseline vectors are needed for three axis attitude estimation. In order to construct these two vectors using differential GPS carrier phase measurements, three antennas (A , B and C) must be used. Since three antennas are available, three vectors can be determined providing a more accurate attitude estimate than if only two of the three were used because the CDGPS errors among the three are independent.

The three CDGPS-measured relative distances between antennas are

$$\begin{cases} {}^{ECI}R_1 = {}^{ECI}Q^{ECEF} \cdot {}^{ECEF}r_{AB} \\ {}^{ECI}R_2 = {}^{ECI}Q^{ECEF} \cdot {}^{ECEF}r_{AC} \\ {}^{ECI}R_3 = {}^{ECI}Q^{ECEF} \cdot {}^{ECEF}r_{BC} \end{cases} \quad (24)$$

where r_{AB} is the vector between GPS antennas A and B .

The ECI relative vectors can be then be compared with the known relative distances in the Body Centered, Body Fixed (BCBF, or body) system

$$\begin{cases} {}^{BCBF}R_1 = A_B - A_A \\ {}^{BCBF}R_2 = A_C - A_A \\ {}^{BCBF}R_3 = A_C - A_B \end{cases} \quad (25)$$

where A represents a known antenna position.

The problem is then to find the DCM, ${}^{BCBF}Q^{ECI}$, that converts from the body coordinates to ECI coordinates for absolute attitude determination, or alternatively ${}^{BI}Q^{B2}$ that converts from one spacecraft body to another for relative attitude determination. These two attitude-estimation approaches are described in the following subsections.

Markley describes several attitude estimation algorithms, any of which would be appropriate for the CUSat application.¹ The Singular Value Decomposition (SVD) method provides an effective attitude estimation scheme for small satellites. Although slightly more computationally intensive than other methods, SVD provides increased stability, scalability and robustness.

While SVD is adequate for understanding the concept of attitude estimation, it does not necessarily provide the optimal result for a time-varying system. Using a Kalman filter will produce the optimal attitude estimation, but describing that implementation in detail is beyond the scope of this paper. By analyzing the presented results, this paper establishes general design guidelines for implementing the proposed attitude-determination approach.

5.1. Absolute Attitude

An exclusively GPS based absolute attitude solution can be obtained by utilizing both pseudorange and carrier phase based navigation solutions. As mentioned previously, the pseudorange based solution generates a line of sight vector from a GPS receiver to a GPS satellite. While the magnitude of this vector is only known to within a few meters, the direction is known very accurately.

Likewise, the direction of the line of sight vector from the center of the Earth to a spacecraft is known very accurately in ECEF. This direction, combined with the CDGPS-generated relative vectors between GPS antennas on a spacecraft can be used to generate an absolute attitude solution.

To compute absolute attitude, vectors R_1 , R_2 and R_3 in the body and inertial coordinates are used to compute the Davenport attitude matrix, B . The Davenport attitude matrix is

$$B = \sum_{i=1}^n a_i \cdot {}^{BCBF}R_i \cdot {}^{ECI}R_i^T, \quad (26)$$

where only the three relative GPS antenna vectors are used. The coefficients a_i are scaling factors used to account for possibly different spacing between antennas. These weighting coefficients normally capture the relative precision of the vectors, and the same is true here: longer-baseline vectors wash out the CDGPS errors more, leading to more trustworthy vector measurements than their shorter counterparts.

Unitary matrices U and V are determined by computing the SVD of the Davenport attitude matrix such that

$$B = U \Sigma V^T. \quad (27)$$

Per Markley, U and V can be used to find the DCM ${}^{BCBF}Q^{ECI}$ from

$${}^{BCBF}Q^{ECI} = U \begin{bmatrix} 1 & 0 & 0 \\ 0 & 1 & 0 \\ 0 & 0 & \det(U)\det(V) \end{bmatrix} V^T \cdot 1 \quad (28)$$

5.2. Relative Attitude

For relative attitude determination, only the vectors generated by the CDGPS algorithm are required. A similar approach to that used in Section 5.1 uses the CDGPS vectors from spacecraft α , $R_{\alpha 1}$, $R_{\alpha 2}$ and $R_{\alpha 3}$ and spacecraft β , $R_{\beta 1}$, $R_{\beta 2}$ and $R_{\beta 3}$ to compute relative attitude. The relative attitude can be reconstructed by forming Davenport's attitude matrix as:

$$B = {}^{ECI}R_{\alpha 1} \cdot {}^{ECI}R_{\beta 1}^T + {}^{ECI}R_{\alpha 2} \cdot {}^{ECI}R_{\beta 2}^T + {}^{ECI}R_{\alpha 3} \cdot {}^{ECI}R_{\beta 3}^T \quad (29)$$

Using the same method as discussed with Equations 26, 27, and 28 a DCM from the ECI coordinates of body α to the ECI coordinates of body β , ${}^{ECI\alpha}Q^{ECI\beta}$ can be constructed. ${}^{ECI\alpha}Q^{ECI\beta}$ merely represents the rotation from one body's coordinate system to another, so it can also be expressed as ${}^{BCBF\alpha}Q^{BCBF\beta}$. The transpose of ${}^{BCBF\alpha}Q^{BCBF\beta}$ provides ${}^{BCBF\beta}Q^{BCBF\alpha}$, the DCM that converts from body α to body β .

Since relative attitude is constructed using noisy vectors in both coordinate systems, the relative attitude accuracy will have roughly double the mean error and variance of the absolute attitude solution.

5.3. Attitude Estimation Simulator

The accuracy results from the CDGPS algorithm can be used to simulate attitude estimation error. A MATLAB script was used to assess pointing accuracy. Three equidistant vectors for a particular body frame and an arbitrary rotation matrix is used to produce a second reference frame. A Monte Carlo simulation can then be used, where error is introduced to the reference frame vectors, to compute an estimate of the rotation matrix ${}^B\hat{Q}^R$. Pointing error can be computed by comparing the true rotation matrix to the estimate.

Using an estimate of 7.5mm 3σ CDGPS error, a 10,000 iteration simulation was run, with an antenna spacing of 25cm. The error is shown below in Figure 5. The mean error is 2.0327 degrees and the standard deviation of error is 0.8837 degrees.

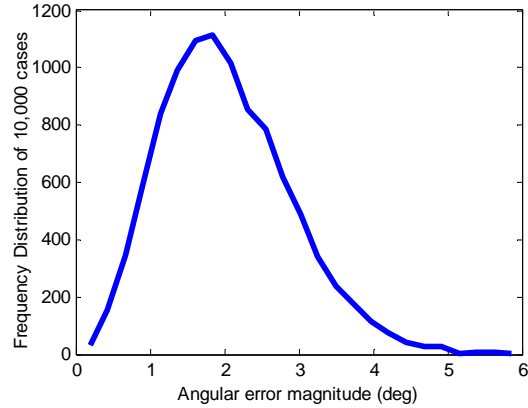


Figure 5. Simulated Angular Error

6. Antenna Placement

Small spacecraft, such as CUSat often use patch antennas for their compact size. Several factors regarding the placement of these antennas can influence the effectiveness of CDGPS based attitude determination. These include phase center variation, antenna field of view, number of baseline vectors, antenna spacing, and integration into a small satellite.

The true position of an antenna in ECEF corresponds to its electrical phase center. This phase center is not necessarily the physical center of the antenna.¹⁰ Additionally, the phase center changes with attitude. While it is possible to calibrate each antenna to determine its true phase center as a function of attitude, this process adds significant complexity to a system which is otherwise free of calibration.

Antennas from the same manufacturer typically have similar phase center characteristics. Therefore, only one model of antenna should be used so the errors due to phase center variation in each antenna cancel out in the double difference.¹⁰ If these antennas are placed on the same face of a satellite, and placed in the same orientation, the error introduced by the antenna phase center variation should be eliminated in the use of both single and double differenced carrier phase measurements. This cancellation occurs only for fixed antenna positions. Phase center error will not be eliminated if two antennas move relative to one another.¹⁰

As mentioned previously, more mutually tracked satellites across GPS receivers improves system performance. Therefore, it is important that all antennas used in the CDGPS solution have very similar fields of view. Placing all antennas on the same face of a spacecraft can accomplish this goal, but care must be

taken to ensure that other parts of the spacecraft do not obstruct the field of view differently for each antenna.

In addition, adequate ground planes should be provided for each antenna. An insufficient ground plane can negatively affect antenna radiation pattern and gain.¹¹ Having different radiation patterns may result in a GPS satellite being visible to one antenna, but not another. Ground plane requirements for a specific GPS antenna model should be available from the manufacturer. However, a general consideration is that sufficient surface area around the mounted GPS antenna must be allotted to ensure maximum performance.

In general, with N antennas, there are $N(N-1)/2$ possible independent vectors can be used for attitude estimation. Adding more antennas to a spacecraft will reduce attitude estimation error. Moreover, adding sets of GPS antennas to different panels of the spacecraft enables pointing flexibility. As a result, the spacecraft can operate in multiple orientations while retaining adequate GPS satellite visibility.

The attitude estimation accuracy as a function of the number of baseline vectors is shown in Figure 6. This result is based on the formulation described in Section 5.3. These simulations assume 7.5mm for the 3σ CDGPS error and equal spacing of 25cm between all three antennas.

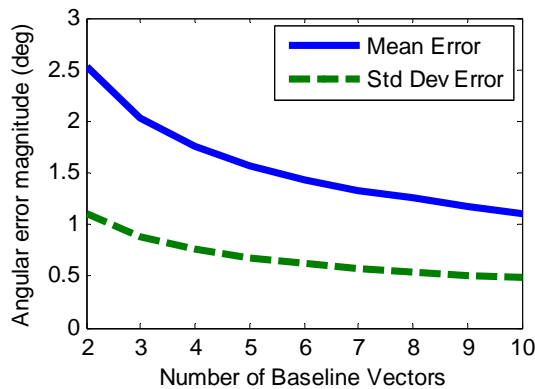


Figure 6. Attitude Estimation Error vs. Number of Baseline Vectors

Notice that attitude estimation accuracy can be further improved by adding antennas. Although such a benefit increases computational expense, it may provide increased pointing accuracy for missions that require it.

Although there are benefits to increasing the number of GPS antennas, it is important to consider the associated disadvantages. One such drawback is the corresponding increase in computational expense as more CDGPS solutions are generated. External surface area for small

satellites is limited. Solar cells, communication antennas, GPS antennas and deployables compete for space. Moreover, using additional GPS receivers would simultaneously increase power consumption and decrease internal space.

For short baselines (such as antennas placed on the same satellite) CDGPS error remains constant with distance. The closer antennas are placed to one another, the higher percentage of error in the relative vector between them. Therefore, increasing the spacing between antennas increases the accuracy of the attitude solution.

In order to quantify the effect of antenna spacing on angular error, a Monte Carlo simulation was run on various GPS antenna spacings, as shown in Figure 7. These simulations assume 7.5mm for the 3σ CDGPS error and equal spacing of 25cm between all three antennas.

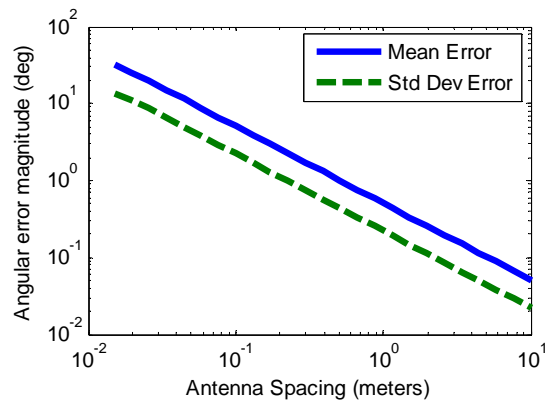


Figure 7. Angular Error as a Function of GPS Antenna Spacing

Even with small antenna spacing (0.25 meters), an instantaneous set of measurements can provide pointing accuracy within a few degrees. These results scale linearly with standard deviation of CDGPS error.

7. Orbit and Pointing Considerations

In designing a GPS-based attitude system for small satellite missions, orbital parameters and attitude pointing schemes must take into account the visibility of the GPS constellation. In a LEO environment, the only orbital parameter that strongly influences GPS satellite visibility is inclination. For the purposes of this discussion, satellite pointing is defined in terms of the direction of GPS antenna pointing.

7.1. Inclination

GPS satellites occupy six orbital planes, at an inclination of 55 degrees.¹² One might expect that orbits with higher inclinations will suffer from poor GPS satellite visibility. To investigate this effect, equatorial and polar orbit scenarios for a zenith pointing spacecraft were simulated using the Spirent GSS7700 GPS simulator. Figure 8 and 9 show the number of visible satellites generated in these simulations. The thick dashed line indicates the minimum number, five, for the proposed CDGPS algorithm. All results assume that the spacecraft in question is in a circular orbit at an altitude of 622 km.

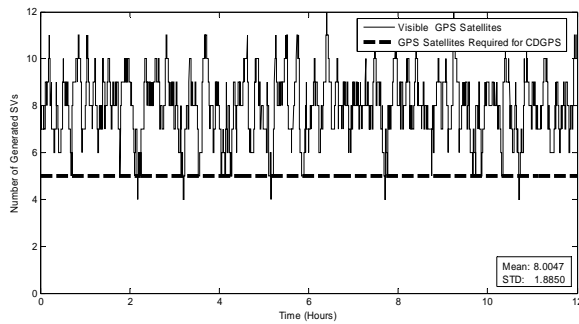


Figure 8. GPS Satellite Visibility for a Zenith Pointing Spacecraft in an Equatorial Orbit

As expected, a more-than-adequate number of GPS satellites is visible on average in an equatorial orbit, as evidenced in Figure 8. Only infrequently does the number drop to four. The equatorial simulation results serve as a baseline for the inclination effect analysis.

Figure 9 shows that the GPS satellite visibility for the polar orbit simulation is similar to that shown in the equatorial orbit simulation. Very rarely does the number of visible satellites drop to three.

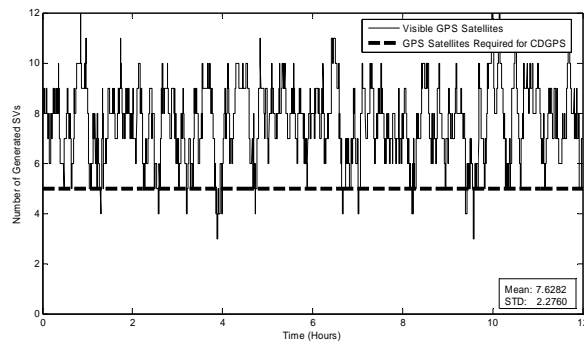


Figure 9. GPS Satellite Visibility for a Zenith Pointing Spacecraft in a Polar Orbit

These simulations show that even with orbits at inclinations greater than 55 degrees, a sufficient number of GPS satellites are in fact visible. This is a result of the small semi-major axis of a LEO spacecraft compared to the large semi-major axis of the GPS constellation, allowing spacecraft over the north and south poles to still see high elevation satellites. These simulations show that for a zenith-pointing spacecraft in LEO, 5 GPS satellites will be seen for 98% of the orbit.

7.2. Attitude

GPS visibility is highly dependent on spacecraft attitude. A zenith-pointing attitude minimizes the potential for Earth obstruction of GPS satellite signals because the GPS antennas are always pointed away from the surface of the Earth.

An inertially fixed orbit will always have some degree of Earth obstruction. The amount of this obstruction will vary with direction of inertial pointing and may vary with time. As an extreme case, the orbit depicted in Figure 10 was simulated.

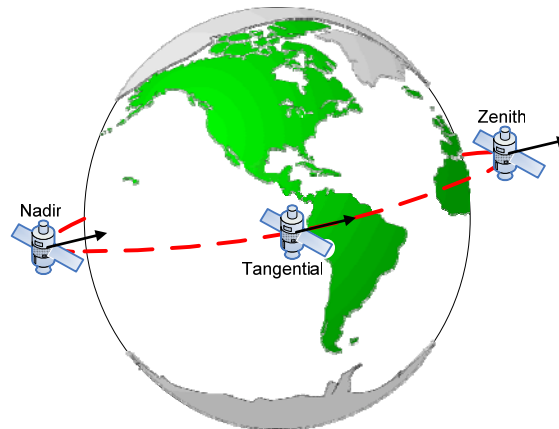


Figure 10. Inertially Fixed Attitude Orbit for GPS Satellite Visibility Study

The GPS satellite visibility of this orbit is shown in Figure 11.

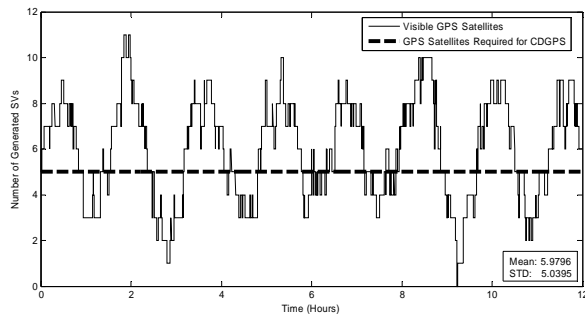


Figure 11. GPS Satellite Visibility for an Inertially Fixed Spacecraft

As expected, the points of maximum visibility in this orbit correspond with the zenith pointing simulations. CDGPS is usable for approximately half of the orbit where the spacecraft is pointed away from the Earth. For the other half, the Earth blocks almost all signals, with the exception of low elevation GPS satellites.

8. CUSat

The Cornell University Satellite (CUSat) project, an entry into the University Nanosatellite-4 Program (UNP-4) is a technology demonstrator for GPS-based attitude determination. CUSat is an end-to-end autonomous in-orbit inspection system, consisting of two functionally identical spacecraft. Both satellites will perform autonomous relative navigation maneuvers to capture imagery of one another using visual-spectrum cameras. These pictures will be telemetered to the ground segment for use in constructing a 3-D model of the target spacecraft.

CUSat is a cooperative inspection system which utilizes GPS data from each spacecraft for both relative navigation and attitude determination. CDGPS provides absolute attitude, relative attitude and relative ranging information, eliminating the need to carry multiple sensor suites.

Three GPS antennas are used to provide three CDGPS relative vectors for attitude determination. The improvement in accuracy gained by using additional antennas does not outweigh the power, space and computing expense, as discussed in Section 6.5. These antennas are mounted on the same surface of the spacecraft as shown in Figure 12.

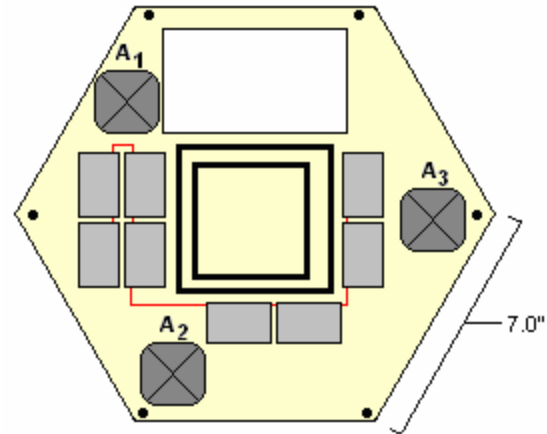


Figure 12. CUSat Top Panel

Three GPS antennas (A_1 , A_2 , A_3) are placed on the top side of a hexagonal spacecraft in order to maximize antenna spacing. Additional surface area surrounding each antenna is reserved to act as a ground plane. The top panel also has a string of 8 solar cells and communication antennas. A portion of the top is left open to provide external access for the camera.

Three COUGAR boards are used in each CUSat satellite to measure GPS data. The COUGAR boards act as sensors to provide data to the Command & Data Handling subsystem (C&DH), which runs the CDGPS, attitude estimation, relative navigation and inspection algorithms. A single processor is used to coordinate each of these algorithms in real time.

The attitude determination system implemented by CUSat employs a Kalman filter. This method provides the optimal estimate for a time varying system and provides additional outputs such as the attitude rate vector and disturbance torque estimates.¹³ The filter will provide accuracy superior to SVD. Using the same method as in Section 5.3, with a CDGPS error of 7.5mm and proper antenna placement, the worst-case instantaneous error was found to be 2.7293 degrees, with a standard deviation of 1.3645 degrees. These results are shown in Figure 13.

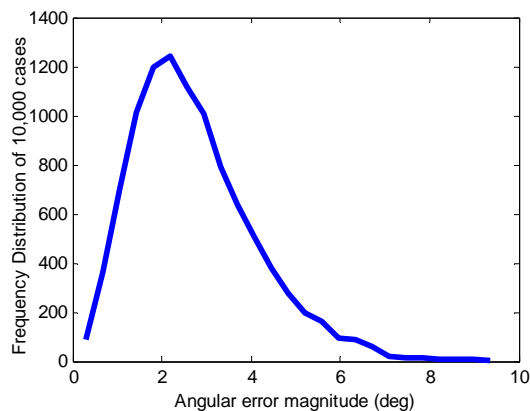


Figure 13. CUSat Pointing Accuracy

Using the Telemetry & Command (T&C) subsystem, both CUSat satellites share GPS data with each other. Through this cooperative process, CDGPS can be used to construct relative attitude and position estimates.

A system must be in place to verify that CDGPS has converged to the correct solution. Without such failsafe checks, the attitude estimate may diverge or become unstable. Since the antenna spacing on each spacecraft is known, this distance can be compared with the vector magnitude produced by CDGPS. If a CDGPS solution is outside 3σ of the actual value, the vector measurement is not used.

A similar method can be used to verify relative ranging vectors between both spacecraft (*A* and *B*). Two CDGPS solutions are computed to form vectors between a single antenna on spacecraft *A* and two antennas on spacecraft *B*. The difference of these vectors represents the vector between the two antennas on spacecraft *B*. If the magnitude of this difference is outside 3σ of the known antenna spacing, the vector measurements are not used.

The optimal CUSat orbit has an inclination of 50 degrees and has an inertially fixed attitude, pointing orbit normal. The orbital parameters are driven by ground station visibility and power requirements. Pointing is driven by power and GPS constellation visibility requirements. Figure 14 shows GPS satellite visibility for an orbit-normal attitude with an orbital inclination of 50 degrees. The resulting visibility is adequate for CDGPS requirements during most of an orbit.

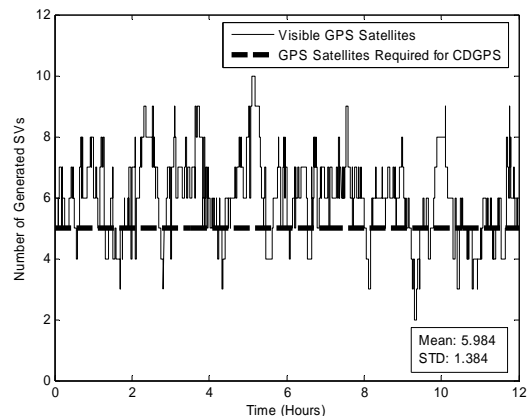


Figure 14. GPS Satellite Visibility for Inertially Fixed Orbit Normal Attitude

On average, CUSat will have 5 visible GPS satellites for 85.76% of the orbit.

9. Conclusions

A GPS-driven system of attitude determination provides many advantages for small satellites. Foremost among these is the high performance-to-cost ratio. The demonstrated low-cost CDGPS implementation offers relative positioning data with an accuracy better than 1 centimeter. This level of resolution enables precise attitude determination, producing an instantaneous pointing accuracy of approximately 2 degrees for an antenna spacing of 0.25cm. Introducing techniques such as Kalman filtering can significantly reduce this angular error, yielding an ADS with excellent performance.

In addition to providing a high performance-to-cost ratio, GPS-based attitude determination offers continuously available coverage in an adaptable, modular package. Simulation results have shown that adequate visibility of the GPS constellation is maintained across the spectrum of LEO altitudes and inclinations, making GPS-based attitude determination a viable option. The accessibility of this solution is further increased as it can be incorporated into small satellites without the need for additional hardware. With only a minimum of 3 GPS antennas, attitude determination with accuracy sufficient for many small satellite missions is attainable. The addition of supplementary antennas, as well as simply maximizing the distance between existing antennas can increase the accuracy of the ADS. The relative independence of a GPS-based ADS from the spacecraft bus offers a nearly calibration-free system that can be easily integrated into a wide variety of satellites without any need for

customization. Furthermore, GPS-based ADS is readily capable of providing multi-body relative attitude and position information, enabling cooperative formation flying operations without requiring hardware modification.

CUSat demonstrates the use of GPS-based attitude determination for a small satellite mission. The CUSat ADS implementation intends to verify, in LEO, that a CDGPS-driven technology can be used for low-cost relative position, relative attitude and absolute attitude determination. If successful, this mission enables advanced applications of GPS-based attitude determination for future small satellite programs.

10. Acknowledgements

The authors wish to acknowledge Bryan Doyle, Joshua Fikentscher and Mason Peck for developing the CUSat ADS architecture. We also would like to thank the Cornell University GPS group for their support and the use of their resources.

11. References

1. Markley, Landis F., "How to Estimate Attitude from Vector Observations," AAS/AIAA Astrodynamics Specialist Conference, pp. 1-19, August 1999.
2. Larson, Wiley J., and James R. Wertz, eds. Space Mission Analysis and Design. 3rd ed. El Segundo, CA: Microcosm P, 1999.
3. Psiaki, M.L., and Mohiuddin, S., "GPS Integer Ambiguity Resolution Using Factorized Least-Squared Techniques," 2005 Flight Mechanics Symposium, October 18-20, 2005.
4. Hofmann-Wellenhof, B, H. Lichtenegger, and J. Collins. *GPS: Theory and Practice* 5th Ed. Springer-Verlag: Wein 2001
5. Mohiuddin, S., and Psiaki, M.L., "Satellite Relative Navigation Using Carrier-Phase Differential GPS with Integer Ambiguities," Submitted for possible presentation at the AIAA Guidance, Navigation, and Control Conf., San Francisco, CA, Aug. 15-18, 2005.
6. Psiaki, M.L., and Mohiuddin, S., "Modeling, Analysis, and Simulation of GPS Carrier Phase for Spacecraft Relative Navigation," Proc. AIAA Guidance, Navigation, and Control Conf., San Francisco, CA, Aug. 15-18, 2005.
7. Kintner, Paul M. "Global Positioning System: Theory and Design." ECE/MAE 415 GPS Course Packet. School of Electrical and Computer Engineering: Cornell University, 2005.
8. Jonge, P.J. de and C.C.J.M. Tiberius, "Integer ambiguity estimation with the LAMBDA method." Proceedings of IAG Symposium on GPS trends in terrestrial, airborne and spaceborne applications. XXI General Assembly of IUGG, Boulder, Colorado, USA (5 p.), July 2-14, 1995.
9. Lachapelle, C. M.E. Cannon, and G. Lu. "A comparison of P code and high performance C/A code GPS receivers for on the fly ambiguity resolution." Bulletin Géodésique 67: 185-192, 1997.
10. Stewart, M.P. "The application of antenna phase centre models to the West Australian State GPS network", *Geomatics Research Australasia*, 68, 61-78, 1998.
11. Bhattacharyya, A. K. "Effects of finite ground plane on the radiation characteristics of a circular patch antenna" *Antennas and Propagation, IEEE Transactions on Publication*, Vol: 38 Issue: 2 p. 152-159 Feb 1990.
12. GPS Joint Program Office. 1997. ICD-GPS-200: GPS Interface Control Document.
13. Humphreys, Todd E. *Attitude Determination for Small Satellites with Modest Pointing Constraints*. Masters Thesis, Utah State Univ., 2003.